Chapter Three - Observing Universal Dynamics

CHAPTER THREE: Observing Universal Dynamics

Discovering the dynamics of the Universe in which we live requires the reliable calibration of distances to galaxies, and reliable estimation of the mean density of the Universe. Unfortunately, estimating the distances to galaxies that are sufficiently remote to be of interest to cosmology is a multi-stage process beset with systematic uncertainties. Of all the fundamental parameters that are significant in astrophysics, the Hubble parameter H_0 and the deceleration parameter q_0 are probably the worst-determined. With new instruments that will become available in the 1980s, some stages of the calibration process may be eliminated, and all stages will be improved. This Chapter describes the main stages in the measurement of the distances and masses of galaxies, and reviews the uncertainties which presently dominate them.

3.1 The distance scale within our Galaxy

3.1.1 The Astronomical Unit

The semi-major axis of the Earth's orbit around the Sun, or the Astronomical Unit (AU), has been inferred with an accuracy of order one part in 10^8 from radar determinations of distances between the Earth and Venus covering a variety of orbital configurations of the two planets. The present best estimate is

$$1 \text{ AU} = 1.49597892(1) \times 10^{11} \text{ m}$$

3.1.2 Trigonometric (annual) parallaxes

Measurements of the annually-recurring part of a bright star's displacement against the apparently fixed mean background of fainter (and generally more distant) stars determines the bright star's trigonometric parallax, π. This angle (in arc seconds) is related to the star's distance d as:

$$\pi = 1/d$$

where d is expressed in units of parsecs (parallax seconds). The parsec is, by definition, 1 AU.cot(1 arc sec), so the value of the AU given in Section 3.1.1 corresponds to

1 pc = 3.0856779×10^{16} m

~6000 known parallaxes. Single-plate errors ~ 0".025 Systematic limits ~ 0".005

Unfortunately, the accuracy of parallax measurements that can be obtained from current ground-based optical telescopes limits the useful range of the parallax technique to <30 pc or so, and only ~~~1000~~ relatively nearby stars are within range of our most fundamental distance indicator.

3.1.3 Moving clusters - the Hyades distance

A star cluster of linear diameter s transverse to the line of sight subtends an angle $\theta = s/d$ when at distance d ($s \ll d$). If the cluster moves relative to the observer, d varies with time and θ changes so that

$$\dot{\theta} = \dot{s}/d - s\dot{d}/d^2$$

If the cluster neither expands nor contracts, $\dot{s}=0$, so

$$\dot{\theta} = -s\dot{d}/d^2 = -sv/d^2$$

where v is the velocity of recession of the cluster (which can be inferred from the mean Doppler shift in the spectra of the cluster stars). Substituting θd for the unknown s, we can write the following relation amongst observable quantities:

$$d = -v\theta/\dot{\theta}$$

The gradient $\dot{\theta}/\theta$ can be found from calibrated photographs of the cluster obtained at a series of different epochs, and the assumption that the cluster neither expands nor contracts can be tested by examination of its distribution of stellar recessional velocities. This procedure for finding d is known as the 'moving-cluster' method.

The only cluster to which both the moving-cluster and parallax methods of distance determination have been extensively applied is the Hyades open cluster. The parallax technique gives the mean Hyades distance as 44.9 pc, while the moving-cluster method gives 48.4 pc. The discrepancy between these values (both independently considered accurate to ~4 pc) probably indicates the absolute reliability of the two techniques at this range.

3.1.4 Main-sequence fitting

Photometric distances to star clusters within our Galaxy but beyond the

range of parallax and moving-cluster methods are calibrated by the technique of main-sequence fitting (spectroscopic parallax). The main-sequence part of the observed colour-magnitude array for the cluster stars is fitted to a standard curve for the main sequence in the colour-luminosity (Hertzsprung-Russell) diagram, using the cluster distance as a variable parameter. To apply this technique successfully, allowance must be made for (a) the effects of interstellar absorption and (b) the effects of stellar evolution, both when establishing the standard main-sequence curve and when comparing it to the data for the cluster whose distance is required.

The existence of a distributed component of the interstellar absorption is inferred from the apparent reddening of the colours of faint stars: the surface temperatures of faint stars implied by their broad-band colours are systematically lower than the temperatures indicated by the ionisation states of elements contributing to their absorption-line spectra. The 'spurious' colour excess E(B-V) increases at about 0.3 magn/kpc. The existence of localised absorbing clouds is obvious from the many 'dark nebulae' seen on large-scale photographs of the Milky Way. At visual wavelengths, the absorption $A(\lambda)$ in magnitudes varies approximately as $\lambda^{-1.2}$ and is attributed to scattering by particles (grains) whose dimensions are of order λ. By comparing the photoelectric spectra of stars of the same spectral type but at differing distances, it is possible to determine the exact form of the absorption law $A(\lambda)$; the classic results of Whitford (Astronomical Journal, 63, 201 (1958)) are shown below

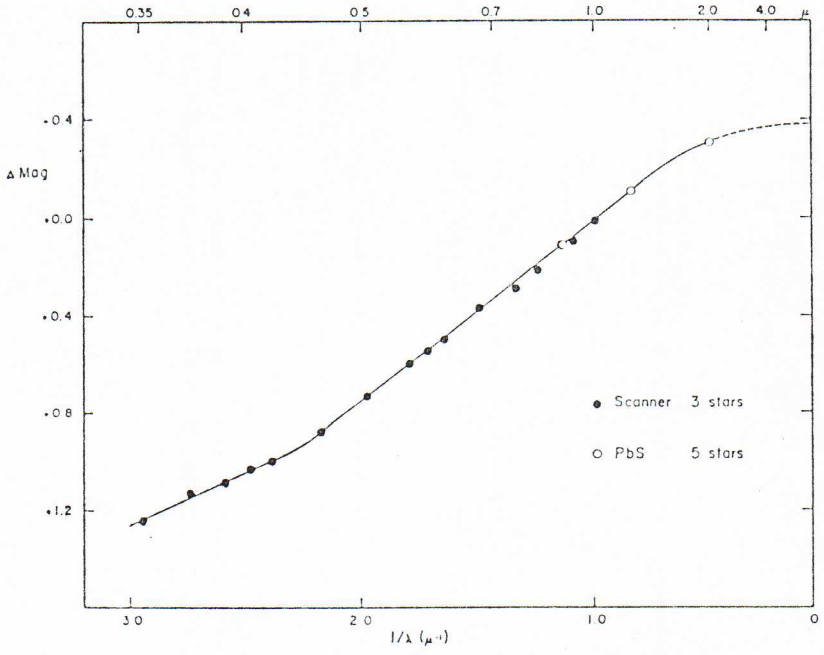

—The reddening-curve derived from observations with a photoelectric spectrum scanner and a lead sulfide photoconductive cell (after Whitford 1958).

Once this $A(\lambda)$ curve is known, the ratio R of <u>total</u> absorption at one wavelength λ_1 to the <u>differential</u> (selective) absorption $A(\lambda_1)-A(\lambda_2)$

$= E(\lambda_1, \lambda_2)$ between two wavelengths λ_1 and λ_2:

$$R = A(\lambda_1)/E(\lambda_1, \lambda_2)$$

can be deduced. The numerical value of R depends only on the form of the absorption curve, not on the distance to the stars involved. Once an observed $A(\lambda)$ curve has been used to calibrate R for a given pair of filters, measurements of the observed colour 'excesses' E can be converted to estimates of the total absorption for stars of unknown distance. Whitford's results gave $R(V) = A(V)/E(B-V) = 3$ for observations through the standard B and V filters, and this value of R is widely used. This use of a single value of R(V) is undoubtedly an over-simplification however, as we can expect the form of the absorption curve to vary around the Milky Way if the composition and sizes of interstellar grains vary with position in the Galaxy. The appropriate value of R must also depend to some extent on the spectral types of the stars being studied, as this will affect the distribution of their light within the B and V filter passbands.

The standard main-sequence curve should be calibrated from a cluster whose colour-luminosity array is not seriously affected by either pre- or post-main-sequence evolution (and should be compared with a part of the unknown cluster's main sequence that is also essentially free of evolutionary distortions). The construction of the standard, 'zero-age' main sequence (ZAMS) is not a trivial matter, because no 'perfect' standard cluster with good photometry, accurately known distance, and an absence of evolutionary effects exists. In particular, the only clusters with good photometry of their very young blue main-sequence stars are beyond the range of the parallax or moving-cluster calibrations. Furthermore these clusters are sufficiently young that their reddest low-mass stars are still undergoing pre-main sequence contraction.

The ZAMS is therefore constructed piecemeal in the following sequence. After correcting all relevant data for interstellar absorption, the observed main sequence of the Hyades cluster is used to fix the red end of the standard ZAMS. The Hyades is chosen because its distance is subject to the cross-check noted in Section 3.1.3, and because individual distances can be derived for many Hyades members. The Hyades data are considered reliable over the range $+0.2 < (B-V) < +1.0$. The Hyades curve is then fitted to the observations of the Pleiades by adjusting the assumed Pleiades distance. A good fit can be obtained redwards of $(B-V)=+0.4$, but bluewards of this value the Pleiades curve lies below that of the Hyades; this difference can be attributed to the effects of evolution in the bluer Hyades stars; the Pleiades curve is therefore used to define the ZAMS down to $(B-V) = +0.1$ (see diagram below)

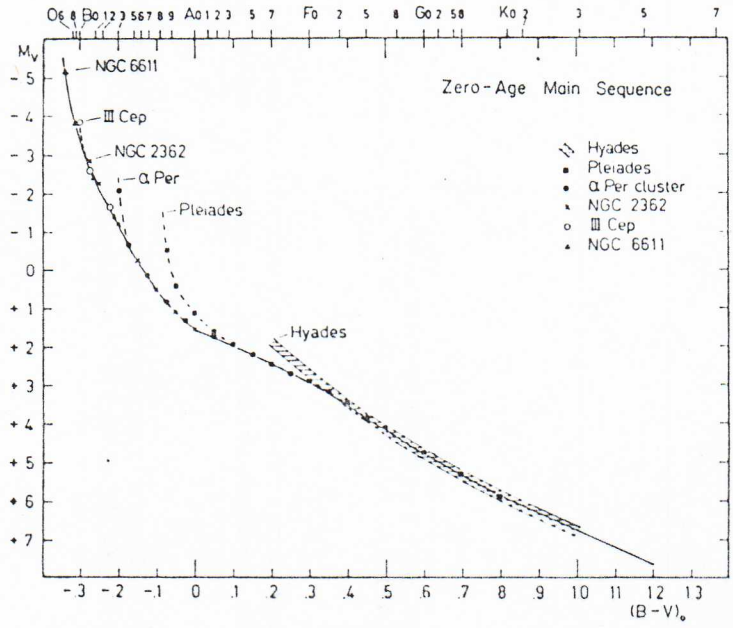

—The zero-age main sequence ("ZAMS") for visual absolute magnitudes, as defined by the non-evolved parts of the main sequences of the clusters indicated in the diagram.

This process is then continued, using in turn the α Persei cluster, NGC 2362, the III Cep Association, and NGC 6111, for which good photometric data are available, to calibrate successively bluer sections of the ZAMS. The procedures and the data are described in detail by Blaauw in 'Basic Astronomical Data', ed. K.Aa.Strand (1963).

The principal weakness of this procedure is the emphasis that it places on the Hyades as the fundamental reference. There is now some evidence that the Hyades stars may be unusually metal-rich, so that their main sequence could be 'too bright' at a given colour by ~0.15 magnitudes. The Hyades will probably continue to play a central role in the distance calibration however until the annual parallax method can be extended to more distant objects by a new generation of astrometric instruments, possibly in Earth orbit.

3.1.5 Pulsating variable stars

The next step in the galactic distance scale is the calibration of the luminosities of bright stars which are not on the main sequence but whose astrophysical properties are both standardisable and easily recognisable. As we seek to determine progressively larger distances, we must rely more on the brightest types of star, as the lower main sequences of more distant clusters become ever fainter and more difficult to measure. Pulsating variable stars have played a central role in distance calibrations because they are both bright and easily recognisable by the shapes and durations of their light cycles.

The RR Lyrae stars are globular-cluster variables with periods typically

0.3 to 0.7 days. Although about 4500 are known, all are beyond the range of direct parallax methods, so their distances must be estimated from those of their clusters based on main-sequence fitting. All RR Lyrae stars have the same mean absolute visual magnitude $\langle M_V \rangle = +0^m.5 \pm 0^m.2$

The classical (Population I) Cepheid variables are between 1^m and 6^m brighter than RR Lyrae stars, so can be detected more easily at great distances. Their greater luminosity makes them a crucial stepping-stone in obtaining photometric distances to nearby galaxies, whose RR Lyrae stars are generally too faint to be recognised reliably or accurately photometered. Unfortunately, the luminosity at mean or maximum light of a classical Cepheid increases with the period of the pulsational variations, so it is necessary to contruct a period-luminosity calibration curve for these stars, rather than simply to use a standard average luminosity as for the RR Lyrae stars. To make matters worse, classical Cepheids are rather rare stars, and only 13 are known in galactic clusters whose distances can be estimated accurately by any of our earlier methods. Two more are probable members of binary systems in which their companion is a star of standardisable luminosity. The basic calibration of the Cepheid period-luminosity relation within our Galaxy therefore rests at present on a very small number of stars; it is shown in the following diagram (from Sandage and Tammann, Astrophysical Journal, 157, 683 (1969))

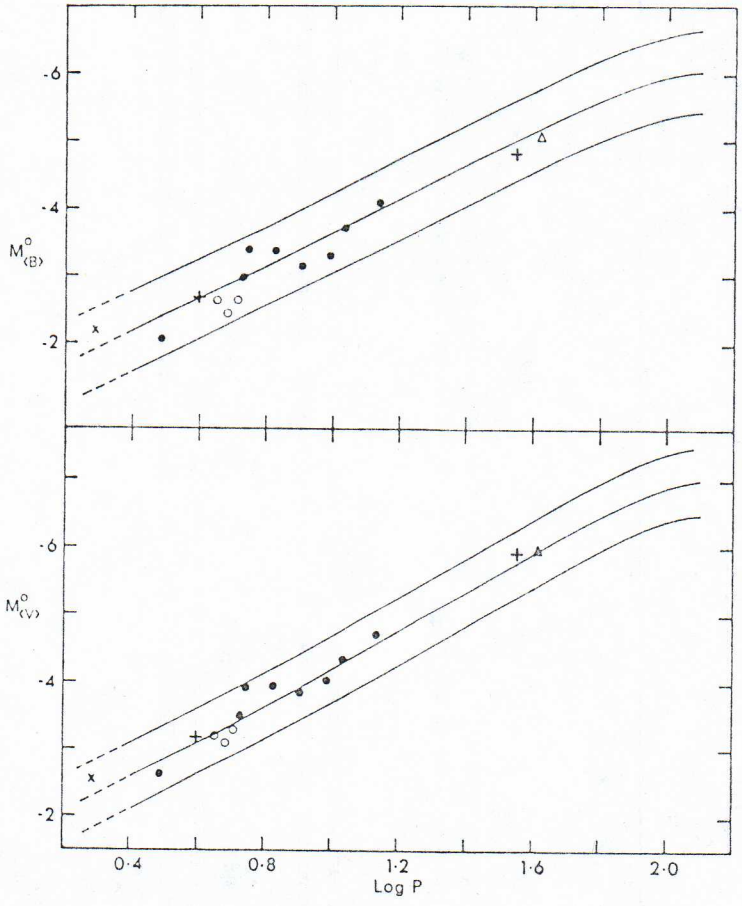

—The *P-L* relation at mean light: *Open circles*, CF Cas and CE Cas *a*, *b*; *triangle*, RS Pup, SU Cas and X; *vertical crosses*, l Car and a UMi. The remaining stars are shown as closed circles.

3.2 Distances to nearby galaxies

3.2.1 Pulsating variable stars

The RR Lyrae stars in nearby galaxies are too faint to be useful as distance indicators except for those in a few nearby dwarf elliptical galaxies in the Local Group, and those in the Magellanic Clouds. The distances of the Large and Small Magellanic Clouds (LMC and SMC), estimated from the apparent brightnesses of their RR Lyrae stars, are 51.3 kpc and 63.1 kpc respectively. These estimates provide a useful check on distances estimated using Cepheid variables.

Over a hundred classical Cepheids in Local Group galaxies have been monitored in several colours; these Cepheids could be used directly to standardise the period-luminosity (P-L) relation if the distances to their galaxies were known by independent methods. The present state of the Cepheid calibration is a compromise that is forced on us by the lack of reliable independent distance indicators within the Local Group. Sandage and Tammann (Astrophysical Journal, 151, 531 (1968)) combined the absorption-corrected data for 94 Cepheids in the LMC, the SMC, M31 and NGC 6822, freely adjusting the assumed distances for these four galaxies to minimise the dispersion around the ridge line of the composite P-L curve, which is shown in the following diagram

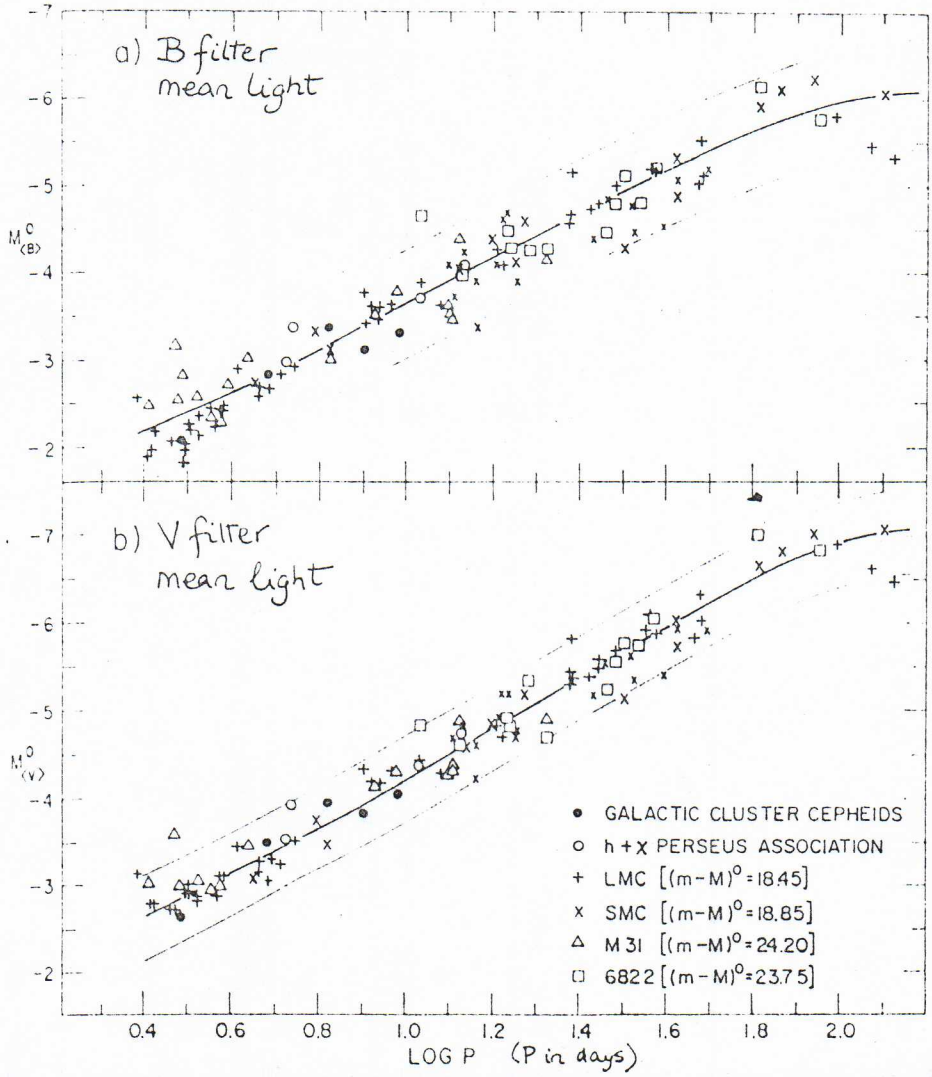

The resulting composite curve was normalised to agree with the limited P-L calibration available from the Cepheids at known distances in our Galaxy (Section 3.1.5). The scatter about the ridge lines of the raw composite curves was $\pm$0.6 magn in B and $\pm$0.5 magn in V; these scatters are considerably larger than expected from observational errors, and imply that there is an intrinsic dispersion in the properties of the Cepheid population, as would be the case if there were further 'hidden' variables affecting the P-L relation.

The theory of the Cepheid pulsation leads us to expect that the P-L relation should depend in detail on the mean colour of the Cepheid, but does not fix the colour dependence quantitatively. Sandage and Tammann (Astrophysical Journal, 157, 683 (1969) and 167, 293 (1971)) constructed empirical P-L-colour and P-L-amplitude curves in an attempt to reduce the scatter in the P-L calibration by admitting further parameters suggested by the theory. The scatter about their final composite P-L-C or P-L-A relations was typically $\pm$0.35 magn. Their suggested Cepheid calibration at mean light in the visual band is

$$\langle M_V \rangle = -2^{m}.459 - 3.425 \log P + 2.52(\langle B \rangle - \langle V \rangle)$$

The accuracy and validity of this Cepheid calibration are still in dispute. The adjusted distances required for the LMC and SMC by Sandage and Tammann to optimise the composite P-L curve were 52.2 kpc and 71.4 kpc respectively. This distance for the SMC disagrees significantly with the distance of 63.1 kpc estimated from RR Lyrae stars. Furthermore, the LMC and SMC are known from radio studies to have a common neutral hydrogen envelope, which would have to be oddly cigar-shaped if the two Clouds are at distances as different as those required by Sandage and Tammann. The assumption that there should be a communal P-L relation for all the Local Group Cepheids is also questionable. For example, many SMC Cepheids have periods in the range 1.5 to 4 days whereas few galactic Cepheids have such periods. The SMC Cepheids are also bluer and larger-amplitude variables than galactic Cepheids of similar period. Such differences raise the possibility that Cepheids in different types of galaxy may not be physically equivalent standards (perhaps due to differences in their chemical compositions), so that attempts to build composite P-L-C or P-L-A relations may be misguided.

3.2.2 Brightest stars in galaxies

Hubble's extragalactic distances were deduced entirely from photometry of the brightest stars in nearby resolved galaxies, and these brightest stars are still important distance indicators today. The brightest stars in galaxies are typically one or two magnitudes brighter than the longer-period Cepheids, so they can be used as distance indicators out to greater distances than can

Cepheids. There are two kinds of problem associated with brightest-star distance scales however. These are problems of recognition (brightest stars may be confused with small stellar groups, with HII regions, or with faint galactic foreground stars) and problems of calibration (the brightest stars are intrinsically rare and statistically extreme classes of object, so it is hard to standardise their calibration against the Cepheid or other distance scales).

The brightest blue stars in nearby galaxies are massive main-sequence stars. Investigations of galaxies in the Local Group whose distances are known from the Cepheid or other calibrations have shown that the luminosity of the brightest blue stars in a galaxy increases with the overall luminosity of the galaxy. Such an effect is to be expected even if all galaxies have the same distribution function for stellar masses, $f(M^*)$. The expected number $N(>M)$ of stars greater than some mass M in a galaxy of N^* stars is

$$N(>M) = N^* . \int_M^\infty f(M^*)dM^* \; / \int_0^\infty f(M^*)dM^*$$

As $f(M^*)$ decreases sharply at high M^*, $N(>M)$ falls rapidly with increasing M. We are therefore more likely to find a star more massive than some high mass M if we survey a galaxy with a larger number of stars N^*. As the total luminosity of a galaxy will be roughly proportional to N^*, while the luminosity of a main-sequence star increases as $\sim M^3$, the brightest stars will tend to be more luminous in the brighter galaxies, even if the stellar populations of all galaxies are identical. Sandage and Tammann (Astrophysical Journal, 191, 603 (1974)) find that the observed blue absolute magnitude of the brightest blue star in each of eleven nearby galaxies could be expressed as

$$\langle M_B \rangle = 0.315\, M_{pg}(\text{galaxy}) - 3^m.48$$

based on their Cepheid calibration. The dispersion in this mean relationship is ± 0.52 magn. Use of this calibration requires photometry both of the brightest blue star and of the total galactic light; the distance must then be chosen so that M_B and M_{pg}(gal) satisfy the above mean relation. A practical difficulty arises from the fact that the brightest blue stars are commonly in open clusters; they are both hard to find and difficult to separate from their cluster.

The brightest red stars are variable supergiants. Although their variability requires that they be monitored carefully before they can be used as distance indicators, their luminosities at maximum light are independent of the luminosity of the parent galaxy. This makes them better standards because they presumably represent a physical upper limit in stellar astrophysics, rather than a purely statistical extremum. Sandage and Tammann find the visual absolute magnitudes at maximum light of the brightest red supergiants in seven Local Group galaxies to be

$M_V(max) = -7^m.9 \pm 0^m.1$

using their Cepheid calibration.

3.2.3 Novae and supernovae at maximum light

The luminosities of novae at maximum light are greater the more rapid the decay of the nova outburst, and empirical relations between decay time and maximum luminosity for the novae in our Galaxy, M31 and the Magellanic Clouds can be used to calibrate photometric distances to other Local Group galaxies whose novae have been sufficiently well observed. A practical difficulty is that novae occur preferentially in the central bulges of spiral galaxies, where high background stellar densities interfere with their detection and with photometry. The most extensive photometric calibration of novae was carried out by Arp (Astronomical Journal, 61, 15 (1960)), who obtained 1000 plates of M31 from June 1953 to January 1955, detecting 30 novae, only five of whose maxima were missed by more than one day. The brightest novae reach maximum luminosities $M_V \sim -8^m$, so this method has a useful range similar to that of the 'brightest-star' method.

Supernovae at maximum light are about ten magnitudes brighter than bright novae, so can recognised in much more remote galaxies. Type I supernovae exhibit a well-defined rise and fall of their light over the first ~60 days of their outbursts, followed by a more gradual decline. The light variations of Type I supernovae are very similar from supernova to supernova; Barbon et al. (Astronomy and Astrophysics, 25, 241 (1973)) show a composite light curve containing data from 38 different Type I supernovae (see diagram).

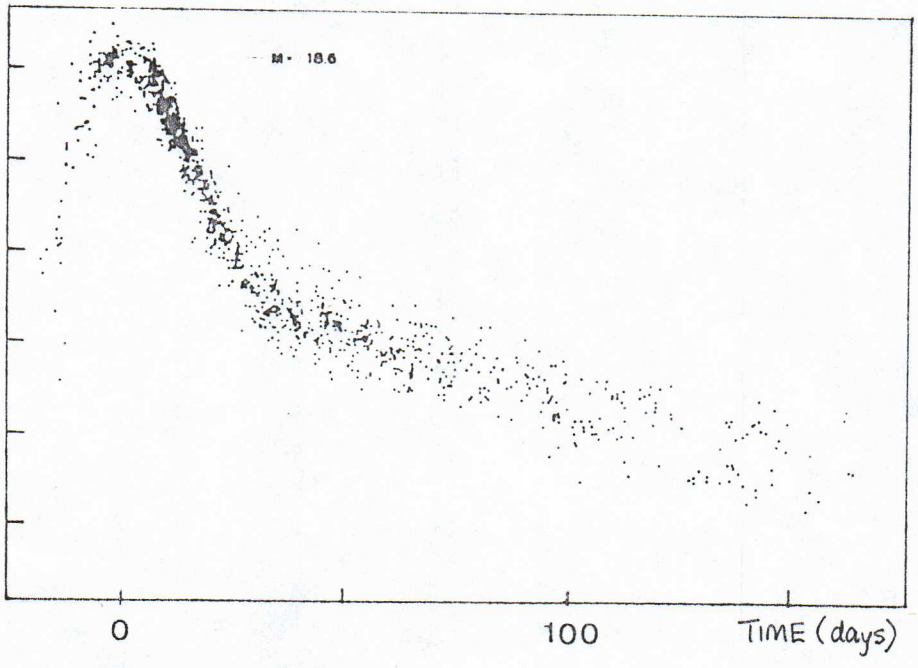

The dispersion around the maximum luminosity is ± 0.7 magn, and could possibly be reduced by subdividing Type I supernovae into 'fast' outbursts with a 2-magnitude decay time of 32 days, and 'slow' outbursts with a 2-magnitude decay time of 38 days. The difficulties in applying the supernova calibration are twofold. First, supernovae occur in a given galaxy only at the rate of one every few decades, so there may be no observations of good quality of supernovae in a given galaxy whose distance is sought. Second, it is difficult to normalise the supernova calibration within our galaxy. The only well-observed Type I supernova in the Milky Way is that documented by Tycho Brahe in 1572. Baade (Astrophysical Journal, 102, 309 (1945)) estimates from Tycho's data that this outburst reached a maximum apparent visual magnitude of $-4^m.0 \pm 0^m.3$. The distance to Tycho's supernova has been estimated from observations of λ21cm absorption lines in the spectrum of its radio remnant, which locate the remnant in the Perseus spiral arm. Uncertainties in the distance and in the correction for interstellar absorption at visual wavelengths (which must be $\sim 1^m.6$) lead to an uncertainty of ± 0.6 magn in the calibration.

Type II supernovae have less well-defined maximum luminosities, although some progress is being made in standardising them using theoretical supernova models (e.g. Schurmann et al., Astrophysical Journal, 230, 11 (1979).

3.2.4 Supernova envelopes

The enormous luminosities of supernovae near maximum light make them attractive candidates as distance indicators, and in recent years several groups have attempted to obtain distances using an approach that avoids the chain of distance calibration discussed so far, and thus avoids the accumulating systematic and random errors that this chain must contain. The method is based on the fact that the continuum emission from supernova envelopes near the maximum of the outburst is approximately thermal (Planckian). The shape of the continuum spectrum can therefore be used to obtain an effective temperature T for the expanding envelope on any given night. The spectra also contain discrete features which can be used to determine the expansion velocity v(t) in the envelope. If v is determined on many occasions, we can calculate the radius of the expanding envelope on any given night:

$$r(t) = \int_0^t v(t)dt + r(0)$$

where r(0) is the (negligible) radius of the envelope soon after the outburst

begins. Knowing the effective temperature T(t), the envelope luminosity follows from the black-body relation

$$L(t) = 4\pi\sigma T^4(t) r^2(t)$$

and the spectral shape can be used to infer the bolometric correction so that the absolute visual magnitude M_V (for example) can be computed. Comparison with the observed apparent visual magnitude at time t then gives the distance to the supernova. The method can be applied over an extended period to give a set of semi-independent distance estimates whose consistency provides a check on the method. The practical difficulties are mainly those in extracting the effective temperature and the expansion velocity from the very complex spectra of the expanding envelopes (see examples in Kirshner and Kwan, Astrophysical Journal, 193, 27 (1974)). The errors and uncertainties in the method have been discussed most recently by Branch (I.A.U. Special Session on Supernovae, ed. D.N.Schramm, p.21 (1978)). The present accuracy of the method is ~25%, and it holds much promise for the future because of its independence from the Hyades-ZAMS-Cepheid distance ladder.

3.2.5 HII region sizes

The sizes of ionised hydrogen (HII) clouds around groups of hot blue main-sequence stars are determined by the total flux of ionising ultraviolet from their exciting stars and by the density of the surrounding neutral gas. The HII regions in a galaxy therefore have a wide range of linear diameters (and shapes) but numerous investigators have attempted to standardise the diameters of the few largest regions in a galaxy for use as distance indicators. HII regions are strong sources of Hα emission and can be separated from the surrounding stellar background using interference filters. The largest HII regions are also more luminous than Cepheid variables, so can be used to extend the range of distance estimates beyond that of the Cepheid yardstick. In principle, HII region sizes might be used for strictly diametric distance estimates that would not need correction for the effects of interstellar absorption. In practice however only a minority of large HII regions in galaxies have sufficiently well-defined outer boundaries to be treated as 'rigid rods' and practical size criteria involve area photometry (e.g. Kennicutt, Astrophysical Journal, 228, 394 (1979)). The irregular shapes and poorly-defined outer boundaries of many HII regions make it advisable to use 'isophotal' diameters $\langle\theta\rangle$ defined by

$$\langle\theta\rangle = 2\sqrt{(\Omega/\pi)}$$

where Ω is the total solid angle subtended by all of the HII region's emission

brighter than some limiting surface brightness F_{min} (watts/m^2/arcsec^2). Isophotal diameters vary with the adopted limiting brightness, but are internally consistent if F_{min} is the same for all measurements. As they are derived from area photometry they define a distance scale that is a hybrid of photometric and diametric measures; at low redshifts this is of no consequence. Kennicutt finds that the mean diameter $\langle s \rangle_3$ of the three largest HII regions in a galaxy increases with the total luminosity of the galaxy according to the relation

$$\log\langle s \rangle_3 = -0.148\ M_{pg}(gal) - 0.268 \qquad (s \text{ in parsecs})$$

This dependence of $\langle s \rangle_3$ on galaxy luminosity occurs for reasons similar to those previously discussed in Section 3.2.2 - the exciting stars of large HII regions are bright blue main-sequence stars whose luminosities determine the sizes of their HII regions if the regions are radiation-bounded. The observed relation between $\langle s \rangle_3$ and $M_{pg}(gal)$ is unfortunately close to the degenerate law

$$\log\langle s \rangle_3 = -0.2\ M_{pg}(gal) + \text{constant}$$

for which the 'HII size' distance to any given galaxy would be indeterminate: if $\langle s \rangle$ increases as $\sqrt{L}$ the angular sizes of HII regions in nearby low-luminosity galaxies would be identical to those in distant high-luminosity galaxies of the same apparent magnitude. This near-degeneracy of the $\langle s \rangle_3$-$M_{pg}(gal)$ relationship precludes the use of HII region sizes alone as distance indicators. Attempts to use them (e.g. Kennicutt, Astrophysical Journal, 228, 696 (1979); Sandage and Tammann, Astrophysical Journal, 190, 525 (1974)) must therefore incorporate some independent indicator of galaxian luminosity into the size calibration. Such independent indicators are based on the integrated properties of galaxies, which form the subject of the next Section.

3.3 Distances to remote galaxies

Photometry of the accuracy necessary to be useful in establishing the distance scale becomes prohibitively difficult for objects fainter than about 22^m. The useful limit of the Cepheids as distance indicators therefore comes at distance modulus (m-M) ~28^m (4 Mpc) for the brightest Cepheids with M ~ -6^m. For the brightest blue stars, this limit can be extended to (m-M) ~ 31^m (15 Mpc), and for supernovae to (m-M) ~ 40^m (1000 Mpc). The upper limits are partly set by image confusion at ground-based limiting resolutions of a few arc seconds, and the advent of the Space Telescope in the mid-1980's will allow the extension of existing techniques to distance moduli of 32^m (25 Mpc) for bright Cepheids, 35^m (100 Mpc) for brightest blue stars, and 44^m (6300 Mpc) for supernovae. The Cepheid and brightest-star methods do not yet allow us to reach the Virgo Cluster (~ 16 Mpc), so for distance estimates to galaxies in the Virgo Cluster or beyond we must either employ distance indicators that depend on integrated properties of whole galaxies, or rely on the supernova calibrations. This Section reviews distance indicators based on whole-galaxy properties.

3.3.1 Luminosity classification of spiral galaxies

It was noted in 1960 by van den Bergh (Astrophysical Journal, 131, 215) that among face-on spiral galaxies whose distances were known the clarity of development of the spiral structure increases with total luminosity of the galaxy. This correlation is presumably indicative of an interaction between the (poorly-understood) astrophysics of the spiral pattern and the total mass of a spiral galaxy. The existence of the correlation makes it possible to estimate the luminosity of a spiral galaxy to within $\pm$ 0.5 magn merely by visual inspection of its image on survey plates. van den Bergh assigned 'luminosity classes' to spiral galaxies on the basis of their appearance on the blue-sensitive plates of the sky survey made between 1949 and 1958 with the 48-inch Schmidt camera at Mt. Palomar Observatory. The nomenclature of his luminosity classes parallels that of the Yerkes classification of stellar luminosities: I for 'supergiant' (highly-luminous) galaxies through V for 'dwarf' (subluminous) galaxies. The following are examples of his criteria, for Sc galaxies: ScI galaxies have long, well-developed and often continuous arms of relatively high brightness, whereas ScIII galaxies have short, patchy arms and ScV galaxies have only a hint of spiral structure in a galaxy of very low surface brightness. The criteria used in making such a classification are complex and hard to quantify; there is obvious scope for subjective bias and systematic differences might be expected in the classifications made by

different observers. It appears however that experienced observers using plates of adequate resolution can achieve remarkable consistency in such purely visual and subjective judgements (see de Vaucouleurs, Astrophysical Journal, 227, 380 (1979), Appendix, for discussion of this point).

The absolute luminosities of galaxies in the different luminosity classes can be calibrated using nearby examples whose distances are known using the standard indicators of Section 3.2. Once such a calibration has been made, photometry of the integrated light of any face-on spiral can be combined with the estimated luminosity to infer its distance. Recent examples of the calibration are given in Sandage and Tammann (Astrophysical Journal, 194, 559 (1974) and de Vaucouleurs in the article cited above.

The luminosity classification of spiral galaxies is also a useful tool for resolving the near-degeneracy in the $\langle s \rangle_3 - M_{pg}$ calibration of HII region sizes (Section 3.2.5). Instead of carrying out the difficult area photometry needed to derive apparent total magnitudes for galaxies, their luminosity class can be used as a substitute for $M_{pg}(gal)$. Although the luminosity classes are not objective continuous variables, so cannot be used for statistical purposes exactly like absolute magnitudes, the $\langle s \rangle_3$ - luminosity class relation has been explored with some success by Kennicutt (Astrophysical Journal, 228, 696 (1979)).

3.3.2 Neutral hydrogen velocity profiles

In 1977 Tully and Fisher (Astronomy and Astrophysics, 54, 661) reported a correlation between the total velocity widths of the 21cm lines emitted by spiral galaxies and their absolute photographic magnitudes as estimated from other distance indicators, after making corrections for the inclinations of the galaxies to the line of sight as discussed below. The physical basis for the existence of such a correlation can be understood as follows.

For many-body bound systems in equilibrium the virial theorem of classical mechanics states that

$$2\langle T \rangle + \langle V \rangle = 0$$

where $\langle T \rangle$ is the time-averaged total kinetic energy of the system and $\langle V \rangle$ is its time-averaged total gravitational potential energy. If Δv is a measure of the spread in velocities among the bodies in the system then $T \propto M(\Delta v)^2$. If all galaxies of a given type had similar mass distributions the total gravitational potential energy in a galaxy of that type would increase as some power of the total mass, M^x, where x would depend on the nature of the common mass distribution. The virial theorem would then imply that

$(\Delta v)^2 \propto M^{x-1}$

i.e. that the velocity dispersion of the matter in a galaxy would be correlated with the total mass of the galaxy, and hence with its total luminosity. Observations of velocity dispersions in within galaxies might therefore be used as quantitative substitutes for the subjective luminosity classification, provided that the type of galaxy under consideration does not have x too close to unity.

The velocity widths measured from the λ21cm radio spectra of spiral galaxies reflect the velocity spread due to differential rotation of their gaseous spiral disks. Obviously the observed velocity width would be zero for a spiral galaxy observed from along its rotation axis, i.e. face-on, and the 'three-dimensional' velocity dispersion Δv_t is equal to the observed dispersion Δv_o only in edge-on spirals. If it is assumed that the disks of spiral galaxies would have circular outlines when seen face-on, the observed axial ratio b/a of the spiral disk would be related to the inclination i of the rotation axis to the line of sight as

$b/a = \cos(i)$, while

$\Delta v_t = \Delta v_o / \sin(i)$

Observations of the axial ratios of spiral galaxies therefore allow their observed velocity dispersions to be corrected for the inclination effect, provided i is not too close to zero, i.e. the galaxies are not too nearly face-on.

Unfortunately the internal absorption in a flat disk of stars and dust of constant thickness would vary approximately as $\sec(i)$, so the dimming of the apparent luminosity of the galaxy by its own interstellar medium should vary as $\sec(i)$. This correction to the total luminosity of a galaxy is small for small i (face-on), but very large for i $\sim 90^\circ$ (edge-on). The galaxies which need the smallest velocity corrections therefore require the biggest internal-absorption corrections before their apparent magnitudes can be used as distance indicators, or their absolute magnitudes can be used to calibrate a velocity width-luminosity relation.

The uncertainties in the determination of the inclination angles i and the uncertainties in estimating the internal absorption corrections are unacceptably large if the galaxy photometry is carried out at blue, visual, or photographic wavelengths. (Similar uncertainties enter into the calibration of the luminosity classification at these wavelengths). An important step towards precise calibration of the Tully-Fisher effect has been made recently however by Aaronson, Huchra and Mould (Astrophysical Journal, 229, 1 (1979)), who used infrared observations at λ1.6μm (H band) for their photometry. At this wavelength the corrections for internal absorption are negligible, even for

edge-on spirals, but the luminosity is due mainly to cool stars rather than to emission from warm interstellar dust, which might not correlate so well as starlight with the total mass of a galaxy.

Aaronson et al. determined apparent magnitudes m_H at H band for the integrated light of their galaxies out to fixed visual isophotal diameters (the necessary detailed area photometry for defining infrared isophotal diameters does not yet exist). They showed that the correlation between infrared absolute magnitudes M_H and the velocity widths Δv deduced by Tully and Fisher was not only better defined than that involving optical absolute magnitudes, but also exhibited a steeper slope, so that the velocity widths are a more sensitive and more accurate indicator of infrared luminosity than they are of visible luminosity in spiral galaxies. This is partly due to the uncertainties in the absorption corrections at visual wavelengths.

The diagram below shows Aaronson et al.'s results for six local spirals whose distances are known from other distance indicators, and their results for 11 spirals in the Virgo cluster and for 18 spirals in the Ursa Major Cluster. The distances to the two clusters are not known absolutely from the primary indicators, but the galaxies within each cluster can be assumed to be all at the same distance from us so their apparent magnitudes are in the same relation as their absolute magnitudes. The mean relation is

$$\langle M_H \rangle (gal) = -21^m.35 - 9^m.5(\log \Delta v_t - 2.5)$$

which corresponds to the power law

$$L_H \propto (\Delta v)^4$$

which would result from x = 1.5 in our earlier discussion.

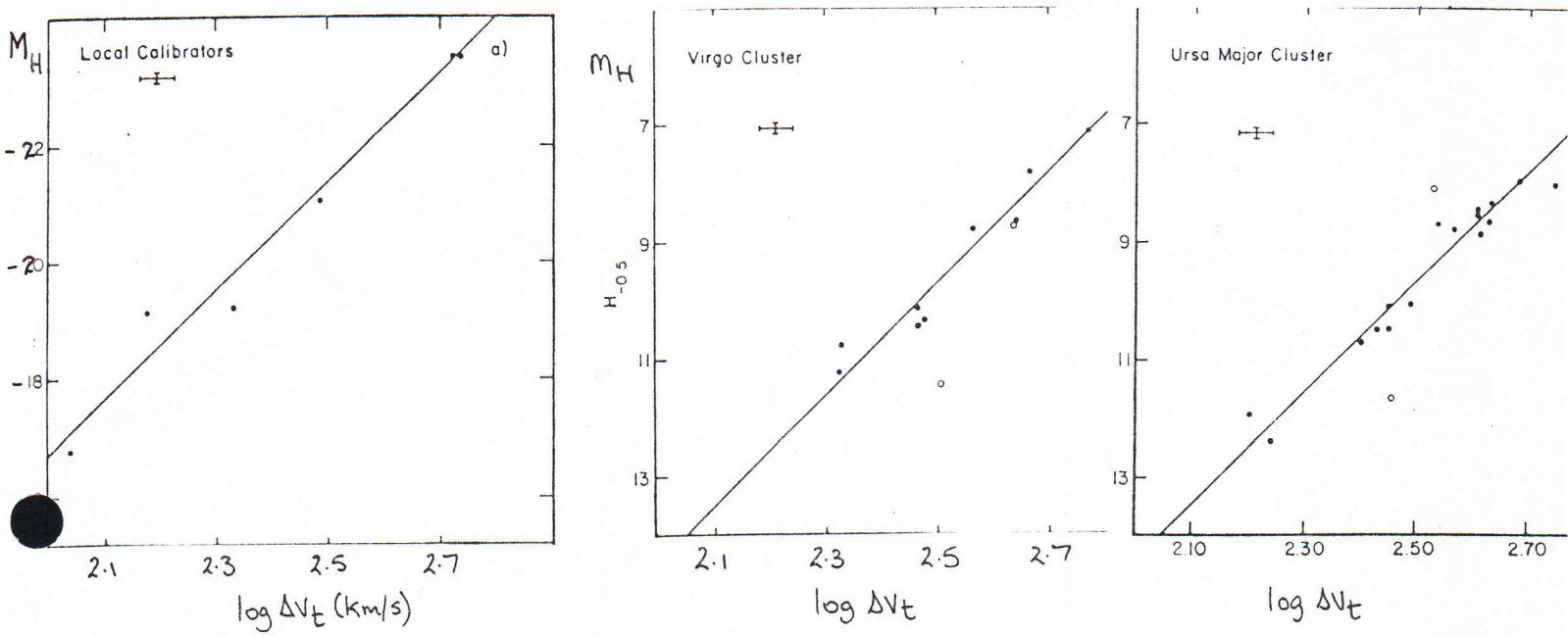

This relationship is significant because x = 1.5 has been found empirically to hold in elliptical galaxies (Fish, Astrophysical Journal, 139, 284 (1964)). This lends support to the idea that the luminosity of spiral galaxies in the H band is due primarily to a massive population of old evolved red stars.

The importance of the relation between the λ21cm line-width and infrared luminosity is that the radio line width provides an objective and quantitative substitute for the van den Bergh luminosity classification, which can be used to standardise the infrared luminosity of a spiral galaxy with negligible corrections for absorption either in the distant galaxy or in our own. The method is easiest to apply to galaxies that do not subtend very large angles at the observer, so that their integrated λ21cm line profile can be determined from a single observation with a radio telescope of modest beamwidth. Once the calibration begun by Aaronson et al. has been refined, the combination of radio and infrared observations of spiral galaxies may provide the best distances to galaxies beyond the range of the Cepheid and brightest-star indicators, and provide a luminosity classification with which to standardise the HII region size calibration. Unfortunately the method cannot yet be applied to elliptical galaxies as they contain too little neutral hydrogen gas and so do not provide strong λ21cm line signals. The only significant uncertainties in the method are the possibility that the measured values of Δv_o depend in detail on the line shapes (which may be affected by tidal interactions between spiral galaxies and their dwarf satellites) and the possibility that the exact form of the correlation depends to some extent on the type of spiral galaxy, requiring a preliminary classification of the galaxy from visual plates before the radio and infrared data for a given galaxy could be used to estimate its distance.

3.4 Estimates of the Hubble parameter

3.4.1 Sandage and Tammann (1975)

At the culmination of a long series of papers on the extragalactic distance scale, Sandage and Tammann (Astrophysical Journal, 197, 265 (1975) concluded that $H_0 = 55 \pm 5$ km/s/Mpc for ScI galaxies in the velocity range 2700 to 21,000 km/s. In an earlier paper (Astrophysical Journal, 196, 313 (1975)), they deduced $H_0 = 57 \pm 3$ km/s/Mpc for a sample of nearby bright spirals ($v < 1995$ km/s); they also found (Astrophysical Journal, 194, 559 (1974)) a value of $H_0 = 55 \pm 6$ km/s/Mpc for galaxies in the Virgo Cluster. They claimed that not only was the global Hubble parameter ~55 km/s, but also that the Hubble flow was isotropic, independent of sample depth, and 'quiet' to within the errors of measurement (mean peculiar velocities of field (isolated) galaxies <50 km/s)). Their error estimates do not allow for possible systematic errors in their distance indicators, which were mainly Cepheids, calibrated through the P-L-C relation (section 3.2.1), HII region sizes estimated visually rather than from area photometry as done by Kennicutt (Section 3.2.4) and a calibration of van den Bergh's morphological luminosity classes, especially the ScI's (Section 3.3.1). The major uncertainties in this process are the Hyades distance, the assumptions made about the global validity of the Cepheid P-L-C relation, the use of subjectively estimated HII region sizes, and the very great weight placed on the nearest ScI galaxy, M101, in the later stages of their calibration. The distances to the M101 group from stellar and HII-region indicators differ by up to 40%. Either M101's largest HII regions are unusually gigantic, or the M101 group is about 20-40% closer than its stellar distance indicators suggest. Despite these uncertainties, the Sandage-Tammann value of H_0 has been extensively used in the literature since 1975. In a subsequent paper (Astrophysical Journal, 210, 7 (1976)), Sandage and Tammann calibrated the Tully-Fisher effect (Section 3.3.2) using photographic absolute magnitudes for their program galaxies, and obtained a value $H_0 = 50.3 \pm 4.3$ km/s/Mpc.

3.4.2 de Vaucouleurs and Bollinger (1979)

An exhaustive study of the extragalactic distance scale and its uncertainties has lead de Vaucouleurs to a radically different value of $H_0 = 100 \pm 10$ km/s/Mpc. His approach differs from that of Sandage and Tammann in that it combines as many independent distance indicators as possible, in the attempt to avoid systematic errors which may be introduced by evolutionary effects, composition variations, or observational error in a distance scale

based too strongly on one indicator. de Vaucouleurs also criticises Sandage and Tammann's use of an average galactic extinction law which vanishes at the galactic poles (as suggested from observations of stellar colours, Section 3.1.4) and instead uses an extinction law derived from counts of galaxies at different galactic latitudes and longitudes. The minimum extinction assumed by de Vaucouleurs for B magnitudes at the galactic pole is 0.3 magn. All of de Vaucouleurs' distance estimates are accordingly lower than Sandage and Tammann's. He also places less emphasis on Cepheid variables and on the M101 Group with its possible large systematic discrepnacies between different indicators, but relies heavily on a subjective luminosity classification for spirals derived from van den Bergh's system. Perhaps the most serious discrepancy with the work of Sandage and Tammann arises from the fact that de Vaucouleurs claims to have detected a significant anisotropy in the apparent value of H_0, which he attributes to a peculiar motion of our galaxy under the gravitational influence of the Local Supercluster.

de Vaucouleurs and Bollinger (Astrophysical Journal, 233, 433 (1979)) examine the values of H_0 derived from observations of 322 spirals with velocities <5760 km/s, and conclude that the Hubble parameter shows significant variations about an all-sky average value of 95 km/s/Mpc. They attribute these variations to a motion of our Galaxy towards Virgo at about 400 km/s, and conclude that when this peculiar motion is subtracted from the analysis by examining directions away from the plane of the Local Supercluster, an asymptotic global Hubble parameter of $H_0 = 100 \pm 10$ km/s/Mpc is deduced. A peculiar motion of our galaxy of this order has also been claimed from studies of the dipolar anisotropy of the 2.7 K background radiation (see Section 4.2.1 below).

3.4.3 Recent results

The trend of recent results is to support the contention of de Vaucouleurs and Bollinger that the local relative velocity field is seriously perturbed by a peculiar motion of our galaxy. Unpublished work by Aaronson, Mould and Huchra, using the infrared-HI width technique described in Section 3.3.2, is reported (Science, 11 January 1980, p.167-169) to have substantially confirmed de Vaucouleurs and Bollinger's velocity anomaly, and to lead to $H_0 = 95 \pm 5$ km/s/Mpc in the asymptotic field beyond the velocity anomaly. If these results are confirmed, observations of distant spirals with Space Telescopes may become critical to the final determination of an accurate, and generally agreed-upon, value of H_0, for only then will it be possible to extend the range of the primary distance indicators to distances beyond those at which the Hubble flow is seriously affected by the local velocity anomaly.

3.5 Classical tests for q_0

In Section 2.5 we derived the 'local' approximation to the Hubble relation for $D_b(z)$:

$$D_b = (cz/H_0).\left\{1 + z(1-q_0)/2 + O(z^2)\right\}$$

which can be combined with the definition of the distance modulus

$$m-M = 5.\log_{10}D_b - \text{const} \quad \text{to give}$$

$$m-M = 5.\log_{10}(cz/H_0) + 5.\log_{10}\left\{1 + z(1-q_0)/2\right\} - \text{const}$$

If $x=z(1-q_0)/2$ is suitably small we can write $(1+x) \sim e^x$, so that

$$m-M \Rightarrow 5.\log_{10}(cz/H_0) + 2.5\ \log_{10}e.z.(1-q_0) - \text{const}$$

$$= 5.\log_{10}(cz/H_0) + 1.086.z.(1-q_0) - \text{const.}$$

Our sensitivity $\Delta(m-M)$ to a given change Δq_0 is therefore

$$\Delta(m-M) = -1.086.z.\Delta q_0 \quad \text{at small z.}$$

At the limit of the Sandage-Tammann ScI sample (z~0.07) this corresponds to a change in apparent magnitude of a standard ScI galaxy by -0.08 magn for $\Delta q_0 = +1$. Such small effects are undetectable in comparison with the intrinsic scatter in our luminosity calibrations, so even within samples of order 100 galaxies at this red shift, the redshift-magnitude relation is sensitive only to gross changes in q_0 ($\Delta q_0 \sim 2$). In order to investigate the value of q_0 sufficiently precisely to constrain cosmological models, we need to work to redshifts > 0.5. At these distances the only galaxies which can be used as distance indicators based on local calibrations are the brightest members of rich clusters, which are normally giant elliptical systems.

3.5.1 Brightest members of rich clusters of galaxies

The basic catalogue of rich clusters of galaxies is that of Abell (Astrophysical Journal Supplements, 3, 211 (1958)) who lists 2712 clusters satisfying well-defined 'richness' criteria documented by the Palomar Sky Survey. To be included in Abell's catalogue a cluster must contain more than 50 galaxies within 3^m of the third brightest member at radii <2 Mpc from the

cluster centre (H_0 = 60). All Abell clusters are also sufficiently distant that the galaxy counts necessary to apply this criterion did not extend over more than one Palomar Schmidt plate; in practice this means that Abell clusters have velocities v > 6000 km/sec.

It has been known for some years that the brightest galaxies in Abell clusters are giant ellipticals whose integrated luminosities do not vary greatly from cluster to cluster; many of these giant ellipticals are also radio galaxies. They are the most massive elliptical galaxies known, and there have been several attempts to calibrate their luminosities for use as distance indicators.

Sandage and Hardy (Astrophysical Journal, 183, 743 (1973)) showed that the luminosities of the brightest galaxies in a sample of clusters with redshifts up to 0.46 correlated with the Bautz-Morgan type of the cluster (Bautz and Morgan, Astrophysical Journal, 162, L149 (1970)). This BM classification is based on the apparent contrast of the brightest galaxy relative to fainter cluster members: BM Type I clusters are dominated ($\langle V_2-V_1\rangle$ = 1.33 magn) by a single central, distended galaxy, often with multiple nuclei (cD galaxy), Type II show less brightness contrast ($\langle V_2-V_1\rangle$ = 0.82 magn) between the brightest and fainter members and the bright galaxy may be a cD or a normal giant elliptical, while Type III do not have noticeably dominant galaxies ($\langle V_2-V_1\rangle$ = 0.37 magn). Sandage and Hardy show that the absolute luminosities of the brightest galaxies in BM Type I clusters are greater than those in Type III clusters by $\langle \Delta M_V\rangle$ = 0.6 magn, but that after allowance for cluster BM type, the mean luminosities of brightest cluster members can be standardised to $\pm$ 0.28 magn. Extension of the redshift-magnitude relation to samples of order 100 brightest cluster members at z ~ 0.5 would therefore in principle determine q_0 to about $\pm$0.05.

3.5.2 K-corrections for giant elliptical galaxies

At the redshifts to which we must work in order to determine q_0, the K-corrections (Section 2.2.2) become important. The K-corrections for giant elliptical galaxies have been investigated by Oke and Sandage and by Whitford, who scanned nearby elliptical galaxies from 3375Å to 11,000Å with apertures of various sizes. They find that there is good consistency among the P(ν) curves for different giant ellipticals, but their results differ in detail due to color gradients across elliptical galaxies (which make the integrated curves somewhat aperture-dependent) and due to differences in their absolute calibration procedures. Obviously the P(ν) curves are flatter in the red (see diagram at end of this Section), so that the K-correction at red wavelengths would be only a slow function of red shift. In contrast, K_B at z=0.25 will depend on the spectrum of a typical giant elliptical in the rocket ultraviolet, while K_V will depend on the rapidly-varying region of the standard galaxy

spectrum near 3900Å.

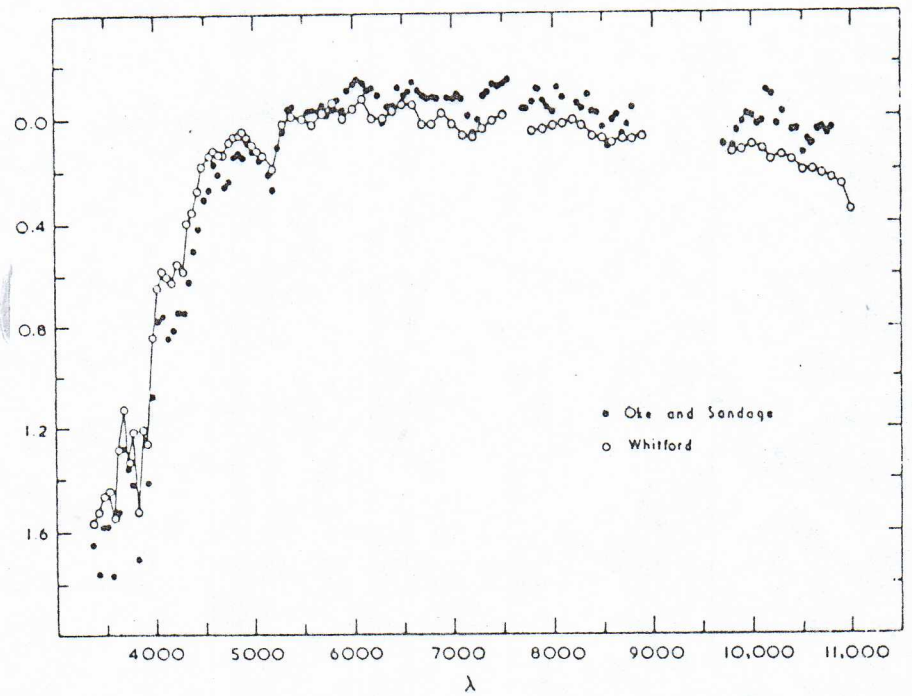

Fig. 1. Intensity distributions in magnitudes per unit wavelength interval for giant ellipticals from the observations of Oke and Sandage (1968) and Whitford (1970).

3.5.3 Aperture corrections

In carrying out photometry of a program galaxy one should collect a fixed fraction of its integrated light with a procedure that does not introduce any distance-dependent errors. Integrated magnitudes determined to a given limiting surface brightness (isophotal diameter) may contain systematic errors for several reasons. The surface brightnesses of images are reduced by absorption in our galaxy, so a given isophotal diameter may correspond to different emitting volumes for sources at different galactic latitudes. Allowance for this effect is complicated by the internal colour gradients in giant elliptical galaxies, by the redshift-dependence of the galaxy colours (K-correction) and by the fact that surface-brightness itself is significantly redshift-dependent at high z (see Section 2.4). A more satisfactory procedure is to measure the integrated magnitude of the galaxy within a given linear radius of its centre (given emitting volume), but this requires adjustment of the aperture size with redshift in accordance with the d-z relation. This in turn requires knowledge of q_0, so photometry through several aperture sizes, and an interative analysis, is needed. Fortunately brightness profiles of elliptical galaxies follow a power-law relation

$L = L_0(r/r_0)^a$, $a \sim 0.5$–0.7, r = aperture radius

so the iteration can be relatively straightforward.

3.5.4 Stellar evolution in distant elliptical galaxies

Far more serious corrections are introduced by the fact that the luminosities of the standard objects themselves can be expected to change with time because of the astrophysical evolution of their stellar populations. The colours and spectra of giant elliptical galaxies show that their light is dominated by an old stellar population composed mainly of red giants. Red giants have essentially the same mean luminosity $\langle L_g \rangle$ regardless of their mass (cf. Section 3.2.2), so the luminosity of an elliptical galaxy at time t will be, to first approximation,

$$L(t) = \langle L_g \rangle . N_g(t)$$

where $N_g(t)$ is the number of giants in the galaxy at time t.

The giants are produced from the main-sequence population which has a number-mass spectrum $N_{ms}(m^*)$ such that

$$dN_{ms} = C.m^{*-2.35}\, dm^*$$

with C a constant. An old galaxy in which main-sequence stars of low mass m^* are evolved to their red giant phase will therefore have many more red giants than will a young galaxy in which only the more massive main-sequence stars have reached their red giant phase. If t_g is the lifetime of a star as a red giant (almost independent of m^*) while t_{ms} is the main-sequence lifetime of the star, the number of giants in a galaxy as a function of time will be

$$N_g(t) = t_g.(dN_{ms}/dt)$$

$$= t_g.(dN_{ms}/dm^*).(dm^*/dt_{ms})$$

where the derivatives are evaluated at the mass m^* which contributes most of the red giants at time t.

For stars of astrophysical age ~10^{10} years (a plausible time scale for the model Universe), the main-sequence mass-luminosity relation is $L_{ms} \sim m^{*5}$, so the appropriate main-sequence lifetime

$t_{ms} \propto m^*/L_{ms} \propto m^{*-4}$, and

$dt_{ms}/dm^* \propto m^{*-5}$ at t~ 10^{10} yr

We can therefore write

$$L(t) = \langle L_g \rangle . N_g(t) \propto \langle L_g \rangle . t_g . m^{*-2.35} . m^{*5} \propto m^{*2.75}$$

where m^* is the main-sequence stellar mass that is making red giants in that galaxy at the time t. Obviously this group has $t_{ms}=(t-t_f)$ where t_f is the epoch of galaxy formation, so

$m^* = (t-t_f)^{1/4}$ and

$$L(t) \propto (t-t_f)^{(2.75/4)} \propto (t-t_f)^{0.7}$$

This calculation indicates what factors have to be known in detail to compute the luminosity evolution of a giant elliptical. It cannot be considered an authoritative calculation, but it serves to show what features of a standard stellar-evolution model would predict how the luminosities of giant ellipticals should increase with time.

Evidently the results of such calculations could be applied only if we knew the time of formation of a given galaxy (did all galaxies form at the same time ?), and if all stars in a galaxy formed together at the time t_f. In fact distant ellipticals have essentially the same integrated colours (after allowing for the K-correction) as nearby ellipticals, so there is little evidence for the predicted time-dependent depletion of the blue main-sequence stars and their replacement by red giants over the look-back times presently available. Whether this lack of colour evolution is due to continuing massive star formation, or to masking of the expected colour changes by other effects, is unclear. The uncertainties in the evolutionary corrections, which some workers put as high as 0.13 magn/10^9 yr, virtually preclude any attempt to determine q_0 by the classical technique using elliptical galaxies. This problem is an example of the deep intermingling of the problems of observational cosmology and extragalactic astrophysics. We will encounter other examples in what follows.

3.5.5 Dynamical friction and cannibalism among the galaxies

The giant cD galaxies which dominate Bautz-Morgan Type I clusters are characterised by high total luminosity, low mean surface brightness, and the frequent presence of multiple nuclei (Rood and Leir, Astrophysical Journal 231, L3 (1979)). These properties together with the observation that they appear to be brighter at the expense of the brightness of their neighbours (Sandage and Hardy, Astrophysical Journal, 183, 743 (1973)) suggest that the cD galaxies may evolve by accreting their smaller neighbours - a process that is becoming known as 'galactic cannibalism' (Ostriker and Hausman, Astrophysical Journal, 217, L125 (1977)).

Ostriker and Tremaine (Astrophysical Journal, 202, L113 (1975)) pointed out that massive galaxies moving in a cluster background of intergalactic gas, stars and low-mass galaxies will experience a frictional drag because of the higher-density gravitational wake that will form behind such a moving object. The effect is known as 'dynamical friction' and was first studied in the context of dense star clusters by Chandrasekhar ('Principles of Stellar Dynamics, p.249 (1960)). The frictional deceleration experienced by such a moving galaxy can be written in the form

$$a = -4\pi(G^2 m/v^2).\rho\left[\sqrt{(2/\pi)}.(v/\sigma)^3.\ln(f)\right]$$

where m is the mass of the galaxy, v is its velocity relative to the background density ρ, σ is the three-dimensional velocity dispersion of the background, and f is a scaling parameter - roughly the ratio of scales of the cluster and of the galaxy. For plausible intracluster values the bracket will be ~2.

The frictional deceleration will make the moving galaxy circularise its orbit and spiral slowly into the centre of the cluster, where it either becomes or encounters the massive central galaxy. The effect will occur even if there is no truly diffuse intracluster gas, because the motion of a massive galaxy will induce fluctuations in the background of low-mass galaxies, intergalactic stars and tidally-stripped dark matter that must exist amidst any real assembly of galaxies in a cluster. The recent discoveries of extended intracluster soft X-ray sources by satellite X-ray observatories, and of 'trailed' or 'head-tail' radio galaxies which are found preferentially in rich clusters, both imply however that many rich clusters have extended, hot gaseous atmospheres (haloes) which will accelerate the rate of cannibalism if these atmospheres have masses comparable to those of the visible matter in the clusters.

Ostriker and Hausman (Astrophysical Journal, 217, L125 (1977) and 224, 320 (1978)) have computed how the luminosity distributions of successful 'cannibals' and of the clusters containing them will evolve with time in the presence of dynamical friction and the resulting galactic

cannibalism. The first-order analysis is as follows. Let the cannibal be a galaxy of mass M and characteristic radius R, and the galaxy being eaten be of mass m and characteristic radius r. Then their total energy before merging will be

$$E = -f_1.GM^2/R - f_2.Gm^2/r - GMm/R_i + T$$

where R_i is the initial separation of the galaxies and T is their combined kinetic energy. f_1 and f_2 here are 'shape factors' which will depend on the internal density distributions in the galaxies. The self-energies of the galaxies will dominate this expression, so we will drop the interaction and kinetic energies to first order. If both galaxies are of similar type, their density distributions will be of similar form but different scales so we will have $f_1 \sim f_2$ and $r \sim R.(m/M)^{1/3}$, so that

$$E = - f_1.(GM^2/R).\left[1 + (m/M)^{5/3}\right]$$

We assume that during the merger of the two galaxies no stars or gas are scattered out of the system and that the total energy of the pair before collision appears as the binding energy of the resulting single system. With these assumptions

$$E_{final} = f_1.G(M+m)^2/(R+dR) = f_1.GM^2/R.(1+2m/M).(1-dR/R)$$

Now the initial energy E is almost <u>second</u>-order in m/M, so the final energy must also be unchanged to <u>first</u> order. Putting the mass m = dM, we must therefore have

$$2(dM/M) = dR/R, \text{ i.e.}$$

$$R \sim M^2 \quad \text{for the cannibal.}$$

Given that the luminosity of the cannibal $L \propto M$ if the mass-to-light ratio of the stellar population is unchanged by the merger, the surface brightness F L/R^2 would evolve as

$$F \propto L/R^2 \propto M/R^2 \propto M^{-3}$$

Luminous cannibals therefore become massive distended galaxies of low mean surface brightness, as in fact observed for the cD galaxies. The multiple nuclei found in some cD galaxies can be interpreted as 'undigested lumps' of recent victims, on this picture. More realistic calculations allow for the fact that low-mass galaxies tend to have higher central densities than successful cannibals, so the shape factors f_1 and f_2 would not be the same,

and that mass-to-light ratios of elliptical galaxies appear to increase with luminosity as $M/L \propto \sqrt{L}$ (Faber and Jackson, Astrophysical Journal, 204, 668 (1976)). With these improvements, it is found that R increases more like $M^{5/6}$. Ostriker and Hausman attempt to follow the evolution of successful cannibals numerically, normalising the time scale of their results to the time taken for a galaxy to accrete its first victim. They find that the luminosity of a cannibal grows so that its integrated absolute magnitude increases almost linearly with time (see diagram below)

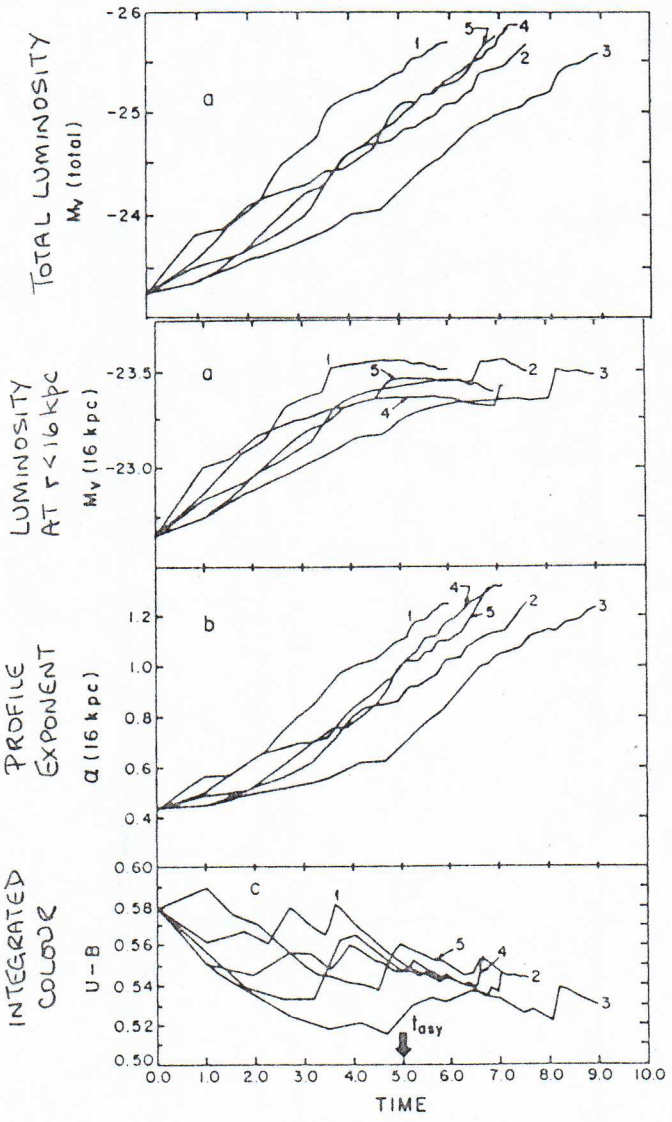

It is important to note that although the total luminosity therefore increases almost exponentially with time, the quantity that is actually measured by observers is the luminosity within an aperture of fixed diameter, which does not. If the luminosity distribution follows the observed power law

(Section 3.5.3)

$L(<r) = L_0(r/r_0)^a$, then

$L(<r) \propto M^{(1-5a/6)}$

so that the luminosity measured through a fixed aperture might increase or decrease with time, depending on the effective value of the exponent a. Ostriker and Hausman compute that a at r = 16 kpc in a cannibal galaxy would slowly increase from its initial value near 0.6 for normal giant ellipticals (Section 3.5.3) until it reaches a value near 1.2 at a time when the cannibal has assimilated about six victims. Beyond this point, their assumptions about the supply of victims are less certain, and they believe that their results may overestimate the subsequent dynamical evolution. At this breakdown point, the luminosity in a fixed 16-kpc radius would be approximately constant as $(1-5a/6) \sim 0$.

The importance of galactic cannibalism to models of the luminosity evolution of the brightest cluster galaxies may be serious if the typical time to accrete the first victim is shorter than the lifetimes of the clusters we are observing by a factor of order 2-10. We need to know much more about the intracluster conditions, and the internal state of the cD galaxies, before the effects of galactic cannibalism on attempts to measure q_0 can be estimated with confidence.

3.5.6 The value of q_0 from the z-D relation

Kristian, Sandage and Westphal (Astrophysical Journal, 221, 383 (1978)) obtained a formal value of q_0, uncorrected for luminosity evolution, of $+1.6 \pm 0.4$ using a sample of 50 brightest cluster galaxies extending as far as $z = 0.75$. They note that their three-colour (BVR) photometry of 33 galaxies gives results consistent with Whitford's K-correction (Section 3.5.2) and that assuming preliminary values of $q_0 = 0$ and $q_0 = 1$ when making the aperture correction leads to final values of q_0 which differ by only 0.2; this shows that a simple iterative procedure for making the aperture correction should in fact be satisfactory. The dispersion around the mean Hubble line is about 0.3 magn in V and in R, consistent with the earlier work of Sandage and Hardy (Section 3.5.1).

The correction for luminosity evolution could however reduce this formal value of q_0 by as much as 1.5, so this data cannot yet distinguish between 'open' and 'closed' Universes with $\Lambda = 0$. Kristian et al. themselves conclude that their results might be used to determine the net luminosity changes due to stellar evolution and dynamical friction, once the value of q_0 has been settled by other means.

3.5.7 The value of q_0 from the z-d relation

The problems of luminosity evolution of the brightest cluster members that were described in Sections 3.5.4 and 3.5.5 have reawakened interest in extracting q_0 from the z-d relation. As discussed in Section 3.5.3, the colour gradients and K-corrections for these objects make it difficult to measure consistent diameters for individual galaxies, and the evolution of the light profiles predicted by the galactic cannibalism theory would further complicate any attempt to use individual galaxy images to define any kind of 'rigid rod'.

Hickson (Astrophysical Journal, 217, 964 (1977)) and Bruzual and Spinrad (Astrophysical Journal, 220, 1 (1978)) have used length scales derived from the distributions of galaxies in rich clusters to define 'standard cluster sizes' which can play the part of rigid rods in defining the z-d relation. Hickson determined the harmonic mean angular separation of the 40 brightest cluster members within a circle of radius 3 Mpc of the cluster centre and showed that this exhibited only a small dispersion from cluster to cluster about a mean value ($H_0 = 50$, $q_0 = 0$) of 1.17 Mpc. He obtained a formal value $q_0 = -0.90 \pm 0.18$ which would require a $\Lambda \neq 0$ model, to account for an accelerating R(t) form.

Bruzual and Spinrad find that this method is very sensitive to the criteria used to identify cluster members and prefer to use a linear scale a derived from analytically fitting the counts of galaxies within annuli of radius r of the cluster centres to a function of the form

$$n(r) = n_0 (1 + r/a)^{-2} + f_0$$

where n is the number of galaxies per unit area of sky, n_0 is a variable central density and f_0 is the number density of background (non-cluster) galaxies. They worked with a sample of 54 clusters out to $z = 0.947$ and derived a mean value of $q_0 = 0.25 \pm 0.5$.

While this method does not suffer from all of the ills which beset the z-D method, it has some of its own. At large distances there may be a tendency to select richer and more concentrated clusters. The K-correction may also influence the measurements indirectly, because spiral and elliptical galaxies are at least partially segregated within rich clusters, the cores being dominated by ellipticals while spirals, if any, prefer the outer regions. The K-corrections for spiral and elliptical galaxies are quite different because spirals contain a young blue population in their disks, so spirals are brightened at large redshifts by the K-correction. Finally, dynamical friction will cause the distribution of galaxies in cluster cores to evolve with time, and should cause apparent decreases in scaling parameters such as a as time

passes in a given cluster. The magnitudes of the accompanying evolutionary corrections to q_0 are less well understood than those arising from luminosity evolution, so the result of Bruzual and Spinrad cannot yet be regarded as a 'clean' estimate of q_0.

3.5.8 The age of the Universe

The only other 'classical' indicator of q_0 that has given even so much as the appearance of a measurement is the comparison between estimates of the astrophysical age of the Universe and of the Hubble time $t_H = 1/H_0$ (Section 2.9). The astrophysical age t_0 can be estimated independently by two indicators : the radiometric age of the chemical elements and the ages of very old star clusters as estimated from the theory of stellar evolution.

The radiometric ages of the chemical elements are esimated from the relative abundances of radioactive parent-product pairs, of which thorium-uranium and rhenium-osmium are the most extensively studied. The interpretation of observed 'whole Earth' and metoritic abundances is fraught with model-dependent assumptions about the formation and evolution of the Earth and of the Solar System, but most workers agree that the apparent radiometric age of locally-available material is in the range 11 to 18 x 10^9 years.

The theory of galaxy formation, which we shall deal with in Chapter Five, suggests that the first globular clusters should have formed within a few x 10^8 years of the onset of the conditions that permit galaxy formation. The ages of the most evolved globular clusters in our Galaxy can be estimated from stellar models, but are sensitive to the assumed internal helium abundance in their stars. The best fits of stellar models to the giant and RR Lyrae regions of the colour-magnitude arrays for old globular clusters require helium mass fractions of 0.25 and ages of 13 to 15 x 10^9 years. The stellar models used for this estimate may however be compromised by the continuing uncertainty surrounding the solar neutrino flux.

The approximate agreement between these two independent, if shaky, chronometers for t_0 suggests however that $t_0 \sim (15 \pm 5) \times 10^9$ years would be a reasonable working estimate.

The Sandage-Tammann value of $H_0 = 55$ km/s/Mpc corresponds to a Hubble time $t_H = 17.8 \times 10^9$ yrs. If $\Lambda = 0$, this clearly favours the regime $q_0 < 0.5$, i.e. an 'open' Universe, although the lower estimates of t_0 would be consistent with a Universe that was just closed. The de Vaucouleurs value of $H_0 = 100$ corresponds however to $t_H = 9.5 \times 10^9$ yrs, barely consistent with the lower estimates of t_0 even if $q_0 = 0$. Substantiation of the de Vaucouleurs value of H_0 would therefore favour a low value of q_0, or require $\Lambda \neq 0$ and an accelerating model for which t_H can be less than t_0. The age estimates therefore appear to be leading us towards stronger constraints than those provided by the observed redshift-distance relations.

3.6 The masses of galaxies and the mean density

The mean density of the Universe is presumably composed of two contributions, the smeared-out mean density of matter in galaxies, and the mean density of matter in any more diffuse or less luminous matter that exists between the galaxies. In this Section we examine what is known about the masses of galaxies, and of the density of intergalactic material.

3.6.1 The rotation curves of galaxies

The most direct approach to galactic mass determinations is to determine the velocity field $v(\underline{r})$ of stars and/or gas in a galaxy and hence to infer the shape of the gravitational potential function $V(\underline{r})$ of the galaxy. This can be matched to models of the internal mass distribution $\varrho(\underline{r})$ which may contain the total mass in a combination of observable parameters. At any radius r in the equator of a galaxy the rotational velocity v(r) satisfies

$$v^2/r = F(r)$$

where F is the net inwards force per unit mass. Except in the inner cores of galaxies, where there may be some pressure support for stars and gas, F(r) is expected to be predominantly gravitational in origin unless the indicator of the velocity field is seriously influenced by large-scale magnetic fields. It will normally be reasonable to put

$$F(r) = - dV/dr$$

where V is the gravitational potential of the galaxy, so that mapping the rotation curve v(r) maps $\sqrt{r.dV/dr}$.

In the ideal application of the rotation-curve method v(r) would be determined sufficiently far from the bulk of the mass of the galaxy that this mass could be treated as a point mass, so that

$$v(r) = \sqrt{(GM_{tot}/r)}$$

i.e. the velocity field would follow the Keplerian $1/\sqrt{r}$ pattern.

In practice however we are generally forced to use velocity indicators sufficiently close to the bulk of the galaxy's mass that the actual mass distribution must be taken into account. Various mass models have been used in the literature to deal with this problem, and there is a good description of the models by Burbidge and Burbidge in Chapter Three of 'Galaxies and the

Universe', ed. Sandage (1975)). Two cases are particularly interesting.

Elliptical galaxies can be modelled to a fair approximation as inhomogeneous spheroids in which the surfaces of constant density are similar concentric spheroidal surfaces. Such surfaces have two equal long axes of length 2a and one short axis of length 2c. If the axial ratio c/a is assumed to be constant throughout the galaxy we can write for the mass dM in the spheroidal shell of semimajor axis x and thickness dx

$$dM(x) = 4\pi(c/a).\varrho(x).x^2.dx, \quad \text{from which}$$

$$v^2(r) = G\int_0^r dM(x)/\sqrt{(r^2 - e^2x^2)} \qquad \left[e^2 = 1 - c^2/a^2\right]$$

$$= 4\pi Gc/a.\int_0^r \varrho(x)x^2dx/\sqrt{(r^2-x^2e^2)}$$

Both the axial ratio c/a and the density profile $\varrho(x)$ can be adjusted to fit this v(r) to the data for a given galaxy. Reasonable decreasing forms for $\varrho(x)$ produce predicted v(r) curves which simulate solid-body rotation $v \propto r$ close to the galactic centres, and evolve to Keplerian laws $v \propto 1/\sqrt{r}$ at large radii.

Galaxies with disklike distributions of stars or gas (spirals and lenticulars) usually exhibit an exponential brightness distribution

$$B(r) = B_0e^{-r/R}$$

within their disks (averaging over all azimuths in the disk to eliminate the details of barred or spiral structure). The corresponding exponential surface density distribution

$$\sigma(r) = \sigma_0e^{-r/R}$$

leads to a simple analytic form for the velocity field in centrifugal equilibrium:

$$v^2(r) = (\pi G\sigma_0r^2/R).(I_0K_0 - I_1K_1)$$

where I and K are modified Bessel functions evaluated at r/2R. The total mass of such an exponential disk is $M_{tot} = 2\pi\sigma_0R^2$. The shape of the predicted velocity curve is shown below:

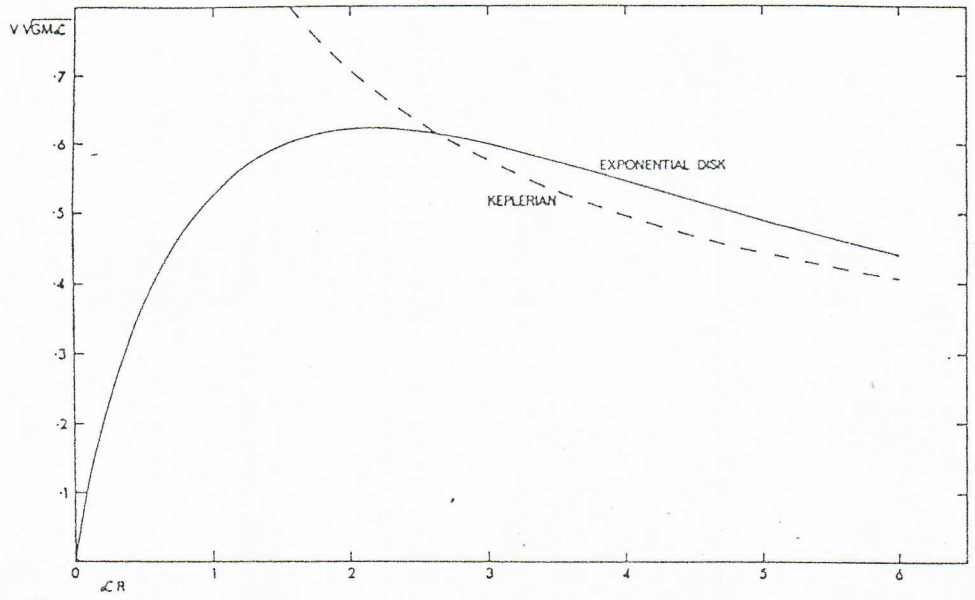

—Dimensionless rotation curve for the exponential disk. The broken line shows the corresponding Keplerian curve.

Most E and S0 and many Sa galaxies have no measurable emission lines in their total spectra, so stellar absorption lines must be used to obtain their rotations. Use of the absorption lines requires a sufficiently long integration time that the continuum against which the absorption lines are to be measured is well-defined. Because the absorption lines originate in a distributed stellar population whose foreground does not in general block off the light from the background, the velocities measured at any given projected radius r' in fact originate at a variety of true radii r. The density distribution $\rho(x)$ must be known before this effect can be corrected for, so the reduction of the data to a rotation curve must be done in an iterative fashion.

The interstellar emission lines from HII regions are easier to use as velocity probes for those galaxies which have significant amount of ionised material. The lines originate in discrete clouds so it is necessary to estimate the correction for projection from the cloud's apparent radial distance r' to the true radial distance r. A problem encountered with the use of optical emission lines is that the HII regions in galaxies tend to be concentrated towards the inner parts of the galaxy, so it is rarely possible to approach the Keplerian region of the rotation curve using such data.

The situation is quite different for the radio λ21cm line emission from galaxies. In spiral galaxies the λ21cm emission can be traced to radii many times the optical radius, so λ21cm studies provide our best opportunity to observe the Keplerian regions. The radio method is largely restricted to spiral and irregular galaxies however, as few ellipticals contain more than about 10^7 solar masses of neutral gas. Recent λ21cm observations made with

very large (≳100-metre) apertures and cooled parametric amplifiers (system temperatures ≲ 40K) have succeeded in tracing the rotation curves of nearby spirals out to radial distances of >30 kpc, e.g. Roberts and Whitehurst (Astrophysical Journal, 201, 327 (1975)), Rubin, Ford and Roberts (Astrophysical Journal, 230, 35 (1979)). It is becoming clear that in most spirals the rotation curves at these large radii are essentially flat, v(r) ~ constant. Such flat rotation curves mean that the inferred total mass is still increasing linearly with radius at the outermost radius sampled (see diagram below)

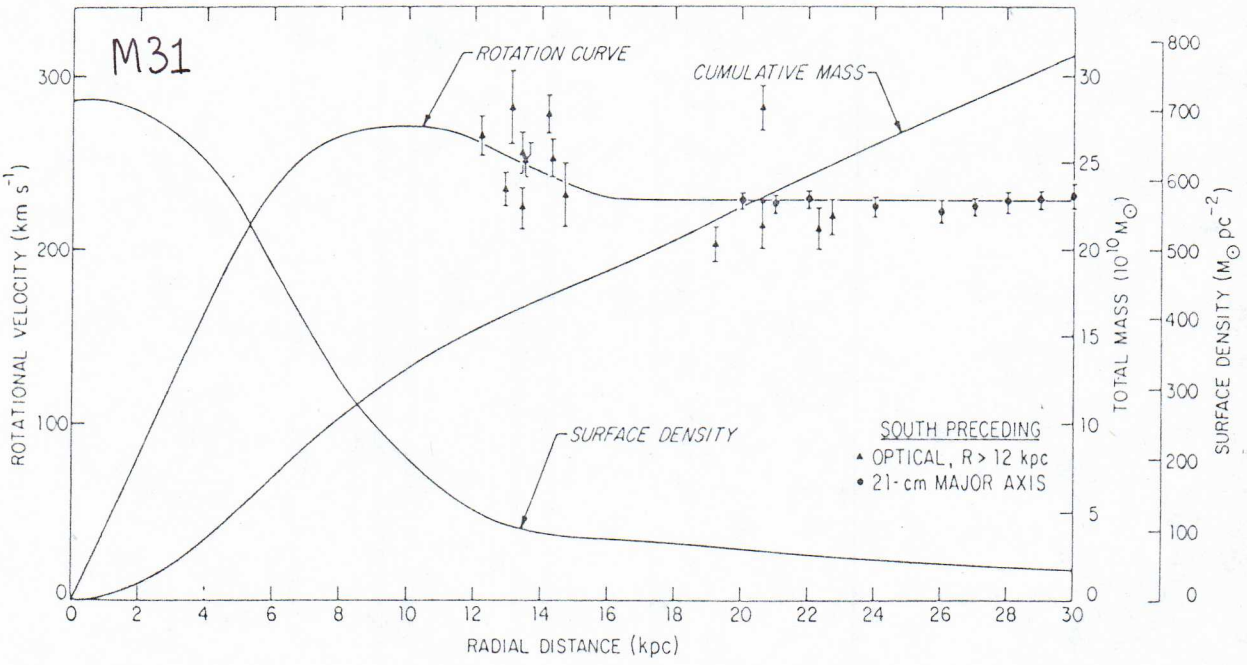

FIG. 16.—The adopted rotation curve, a composite of optical (Rubin and Ford 1970) data and 21-cm major axis measurements. The surface density and cumulative mass curves are for a highly flattened model.

Results such as these imply that the densities in the outer regions of the galaxies studied are falling off only as rapidly as $\rho(r) \propto r^{-2}$, whereas the luminosities fall off as r^{-3} or steeper in the outer parts of spheroidal (elliptical) galaxies and exponentially in disk galaxies. We are therefore forced to the conclusion that the effective mass to light ratio (M/L) increases drsatically in the outer parts of these galaxies because they contain significant amounts of subluminous or dark matter. The spatial distribution and astrophysical nature of this dark matter remain obscure - white dwarfs, red subdwarfs, neutron stars, black holes and massive gaseous haloes are all popular hypothetical candidates.

The rotation-curve methods must today be interpreted as giving lower limits to galactic masses, in the absence of clearly Keplerian regions for most galaxies. Typical lower limits for spiral galaxies are in the range 2 to 4×10^{11} solar masses, though in one case (NGC1961, Rubin, Ford and Roberts, op.cit.) the lower limit is already ~ 10^{12} solar masses. Mass-to-light ratios, typically M/L ~ 10 solar units in the inner regions of the galaxies studied, must increase to M/L ~ 200-300 in the systems with flat rotation curves at large radii.

3.6.2 Binary galaxies

The statistics of occurrence of close pairs of galaxies as a function of galaxy separation show that there are more very close pairs than can be expected from purely random projection in a general field of single galaxies. This observation means that, on a statistical basis, binary galaxies exist, so that we should be able to estimate galaxy masses from observations of the interactions in binary systems. The methods that are used to obtain stellar masses from binary star systems cannot be applied to galaxies, however, because galaxy-galaxy orbit times are much too long for our observations to represent more than a single 'snapshot' of the velocity difference Δv and projected orbital separation d at some unknown phase of the orbit. We can obtain from data the quantity

$$\Delta v^2 d = GM_{tot} \sin^3\theta \sin^2\phi = GM_{tot} \cdot f_p$$

where θ and ϕ are the angles between the line of sight and the plane of the orbit, and between the plane containing the two galaxies and the observer and the normal to the orbit (see diagram below)

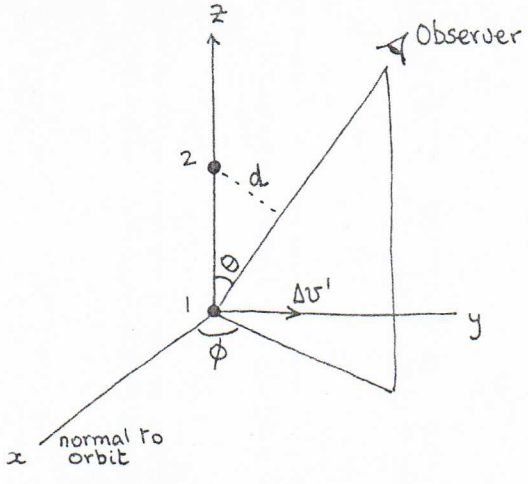

$M_{tot} = M_1 + M_2$

(y,z) = plane of true orbit

$\Delta v'$ = true relative velocity

This relation holds if the orbits are circular and the galaxies interact like point masses (i.e. there are no significant tidal interactions or shape factors influencing the orbital dynamics). For binary galaxies, unlike binary stars, we have no way to determine the projection factor f_p in any individual case, and must assign it the average value expected within a randomly-oriented sample which satisfies the particular selection criteria that have been applied to the actual galaxy sample under study. If there were no bias towards particular values of θ and ϕ in the criteria used to designate particular galaxy pairs

as probable binaries, the projection factor f_p would take its value averaged over the entire sphere, $\langle f_p \rangle = 3\pi/32 = 0.295$. In fact the statistical procedures used to select likely binary pairs for study are biased towards inclusion of pairs of small separation d, so are weighted towards small values of θ and of f_p. Furthermore, whatever method is used to select likely binary systems, some spurious pairs will creep in and these will tend to have large values of Δv. Making allowance for these biases, and for possible ellipticity of the orbits, is awkward and there is still controvery over the best method (see the review by Faber and Gallagher, Annual Reviews of Astronomy and Astrophysics, 17, 135 (1979)).

The merit of the binary-galaxy method is that it can in principle be applied equally to all types of galaxy. Potential problems, other than those associated with selection bias, are the possibility that galaxies do not behave like point gravitating masses over typical binary-galaxy separations (this may be particularly true if galaxies have extensive massive haloes with high M/L ratios), and the assumption that galaxies in binary systems form an unbiassed sample of the general field.

The mass-to-light ratios derived for spiral-spiral pairs in recent years give $\langle M/L \rangle \sim 30$. The data for pairs containing elliptical systems are sparser, but suggest $\langle M/L \rangle$ for ellipticals is also in the range 30-50.

3.6.3 Velocity dispersions in galaxies

For a spherical non-rotating galaxy in equilibrium the gravitational potential energy is given by

$$V = - G \int_0^R M(<r).4\pi r^2.\rho(r).dr/r$$

where R is the total radius, $M(<r)$ the mass within a sphere of radius r. By the virial theorem

$$M\langle v^2 \rangle + V = 0$$

where M is the total mass of the galaxy and $\langle v^2 \rangle$ is the mass-weighted average of the square of the space velocities of the stars relative to the centre of the galaxy. Velocity-dispersion methods of estimating galactic masses replace the integral for V and the $\langle v^2 \rangle$ term by approximations to these quantities that can be derived from observables. The light distribution in a galaxy is used as a first approximation to the mass distribution required to evaluate V (this amounts to the assumption that M/L is constant through a galaxy), and $\langle v^2 \rangle$ is estimated from the observed line-of-sight velocity dispersions (assuming in effect that the velocity dispersion is constant throughout the galaxy). Both of these assumptions are extremely questionable in the light of

data on rotation curves, and the M/L ratios derived from these assumptions are not very reliable, except near galactic nuclei where both assumptions are more likely to be true over regions of restricted scale. M/L values derived from this approach are usually in the range 5-15 (e.g. Faber and Jackson, Astrophysical Journal, 204, 668 (1976)).

3.6.4 Dynamics of groups and clusters of galaxies

Clusters exist on all scales from the rich Abell clusters down to binaries. If it is assumed that most groups are gravitationally bound, the virial theorem can be applied to the motions of the group members. The problems associated with this method are the need to assume preliminary M/L ratios in the galaxies to determine V, the need for the assumption that the groups have reached dynamical equilibrium in the age of the Universe, and the criteria for group membership. The latter is particularly vexing, for if velocity is used as a criterion for group membership, systematic exclusion of high-velocity galaxies will lead to systematic underestimation of the masses of the groups. Typical M/L ratios derived for small groups (Turner and Gott, Astrophysical Journal Supplement, 32, 409 (1976); Rood and Dickel, Astrophysical Journal, 224, 724 (1978)) are in the range 30-100.

When applied to the rich clusters, the virial procedures give $\langle M/L \rangle$ values typically 200-300 (see the review by Faber and Gallagher for details). There is little doubt that the major contributor in the data to such high values of M/L is the large velocity dispersions of many rich clusters (~ 1000-2000 km/s), so the question of whether or not the entire clusters are single dynamical entities is paramount in interpreting this result. If there is significant subclustering within the units that are analysed, the high $\langle M/L \rangle$ ratios could be spurious. Contamination of cluster data by non-cluster galaxies with significantly discrepant velocities may also be a problem.

3.6.5 The mean density in the form of galaxies

Studies of the redshift distributions in catalogues of galaxies that are complete to well-defined limiting magnitudes define the luminosity function $\underline{\phi}(L)$ for galaxies; this function specifies the number of galaxies per unit volume per unit luminosity interval. It can be expressed in the form (Schechter, Astrophysical Journal, 203, 297 (1976)):

$$\underline{\phi}(L)\,dL = \underline{\phi}^* . \exp(-L/L^*) . (L/L^*)^{x} . d(L/L^*)$$

with $x \sim -1$ and $L^* \sim 3 \times 10^{10}\ L_\odot$. Once $\underline{\phi}^*$ is known, we can compute the mean luminosity density in the Universe. A typical recent estimate (Davis,

Geller and Huchra, Astrophysical Journal, 221, 1 (1978)) is

$$\mathcal{L} = 1.2 \times 10^{8}.(H_0/100) \quad L_\odot.Mpc^{-3} \qquad = \int_0^\infty L\,\Phi(L)\,dL = 6\times10^{7}.(H_0/50)$$

The dependence on H_0 arises because the luminosities of galaxies scale as $(H_0)^{-2}$ while the volumes over which their luminosities are estimated scale as $(H_0)^{-3}$.

The mean mass density in the form of galaxies can be estimated from this as

$$\rho_g = \langle M/L \rangle.\mathcal{L} \quad M_\odot.Mpc^{-3}$$

where $\langle M/L \rangle$ is the mean mass-to-light ratio for galactic matter. The discussion in Sections 3.6.2 to 3.6.4 could be used to justify $\langle M/L \rangle$ in the range 30-300, depending on whether one gave more emphasis to the results from small groups of galaxies, or to results from the rich clusters. In most cases, the mass scale is estimated from a quantity of the form $f.\Delta v^2.d$ where Δv is some velocity differential and d is a length scale. The estimates of Δv will not depend on the assumed value of H_0 but those of the length scale will vary as $(H_0)^{-1}$. The scale of galactic masses therefore varies as $(H_0)^{-1}$ while that of luminosities varies as $(H_0)^{-2}$. The deduced $\langle M/L \rangle$ therefore scales as H_0, so the estimate of ρ_g scales as $(H_0)^2$. The M/L ratios quoted throughout this Section have been normalised to $H_0 = 50$ km.s^{-1}.Mpc^{-3}.

normalise all M/L to H_0=100 for later versions

The range of M/L values therefore corresponds to

$$\rho_g = 1.2 \times 10^{-28} \text{ to } 27 \quad (H_0/50)^2 \text{ kg.m}^{-3}$$

Note from equation (2.19) that in a model with $\Lambda = 0$

$$q_0 = (4/3)\pi G \rho_0.(H_0)^{-2}$$

so the contribution to q_0 from the 'known' galaxy density is independent of the assumed value of H_0 and is

$$q_0(\text{gal}) = 0.013 \text{ to } 0.13$$

These estimates of M/L for galaxies therefore favour the 'open' models if $\Lambda = 0$ and if there is no significant contribution to the mean density in forms that have not been counted by the procedures used to deduce $\langle M/L \rangle$.

$\Lambda \neq 0$, these data $\rightarrow$ $\quad -8\times10^{-36}\,s^{-1} < \Lambda < 4\times10^{-36} \quad H_0 = 50 \quad \times\left[H_0/50\right]^2$ to convert